

Poleward Shift and Change of Frontal Activity in the Southern Hemisphere over the Last 40 Years

SILVINA A. SOLMAN

Centro de Investigaciones del Mar y la Atmósfera, CONICET-UBA, DCAO/FCEN, UMI IFAECI/CNRS, Buenos Aires, Argentina

ISIDORO ORLANSKI

Atmospheric and Oceanic Sciences Program, Princeton University, Princeton, New Jersey

(Manuscript received 5 April 2013, in final form 11 October 2013)

ABSTRACT

Several studies have documented the poleward shift of the midlatitude westerly jet of the Southern Hemisphere during the last decades of the twentieth century, mainly during the warm season. In this work the consistency between this change and the seasonal changes in frontal activity and precipitation are explored. The authors also attempt to identify the correlation between frontal activity and precipitation changes.

Frontal activity is defined using the 40-yr European Centre for Medium-Range Weather Forecasts (ECMWF) Re-Analysis (ERA-40) dataset for the period 1962–2001 as the temperature gradient times the relative vorticity at 850 hPa. Considering cyclonic systems only, an enhancement of the frontal activity at high latitudes in the last two decades is apparent. However, the pattern of frontal activity change is not zonally symmetric, with the zonal asymmetries consistent with the climate change signal of the zonal anomaly of the 300-hPa geopotential height.

The pattern of precipitation change, showing midlatitude drying and high-latitude moistening, is consistent with the pattern of the frontal activity change, explaining to a large extent both the zonal mean and asymmetric rainfall changes. This consistency is also found in terms of the year-to-year variability of the zonal mean at both mid- and high latitudes. However, the frontal activity has a complex relationship with rainfall (not every frontal system is associated with rainfall events), and this consistency is unclear over some specific regions.

Results presented here highlight the robust link between the change in the asymmetric component of the upper-level circulation, the frontal activity, and rainfall over the mid- to high latitudes of the Southern Hemisphere.

1. Introduction

The poleward shift of the midlatitude westerly jets and storm tracks in the Southern Hemisphere (SH) during the austral summer months in the last decades has been reported in many articles. Observational studies based on a variety of data sources and based on a variety of metrics of the SH circulation have shown this poleward shift and the underlying mechanisms. Thompson and Solomon (2002) examined recent trends in geopotential height over the periphery of Antarctica from radiosonde data and showed that trends in the SH tropospheric

circulation are consistent with a trend toward the high-index polarity of the southern annular mode (SAM). In particular, they highlighted the impact of the ozone concentration on the SAM trend during the austral summer. Archer and Caldeira (2008) analyzed the upper-troposphere jet streams derived from reanalyses and showed that in the last 30 years the jet streams have risen in altitude and moved poleward in both hemispheres. They also found that in the SH the subtropical jet weakened, whereas the polar jet strengthened during the austral summer. Pezza et al. (2007) explored the association between recent trends in cyclones and anticyclones in the SH with the low-frequency variability of the Pacific Ocean, including ENSO and the Pacific decadal oscillation. Chen and Held (2007) documented the poleward shift of the SH surface westerlies during summer using reanalysis and suggested that this shift is due to an

Corresponding author address: Silvina A. Solman, CIMA (CONICET-UBA), Ciudad Universitaria, Pabellón II-2do. Piso (C1428EGA), Buenos Aires, Argentina.
E-mail: solman@cima.fcen.uba.ar

increased momentum flux in midlatitude eddies with fast eastward-propagation speeds. In a recent study, Fyfe et al. (2012) showed that the observed positive trend during austral summer in SAM over the last half-century resulted primarily from increasing anthropogenic emissions of greenhouse gases and decreasing ozone concentration, with an opposing influence from contributions of anthropogenic aerosols. Moreover, Gillett et al. (2013) showed that the influence of greenhouse gas, aerosol, and ozone changes have distinct significant contributions to observed sea level pressure (SLP) trends over the past 60 years, regarding its zonal, meridional, and seasonal structures, being the combination of both greenhouse gas and ozone changes the drivers of the SAM trend, mainly during the austral summer season. A number of studies based on cyclone-tracking techniques have also shown that the number of cyclones between 40° and 60°S have decreased while increasing poleward of 60°S during the last 30 years (e.g., Simmonds and Keay 2000; Fyfe 2003; Wang et al. 2006). Bender et al. (2012) provided an additional observational support for a poleward shift in storm-track cloudiness.

Several regional studies have also discussed the impact of the changes in the extratropical circulation of the SH during the last decades on the regional climate. Among others, Silvestri and Vera (2003) suggested that the changes in the austral spring season temperature and rainfall over southeastern South America and Antarctica during the 1970s were strongly influenced by the interdecadal variability of SAM. Frederiksen and Frederiksen (2007) discussed the impact of the poleward shift of the storm track after the 1970s on winter rainfall reduction over southwestern Australia. Moreover, Cai et al. (2012) showed evidences of the role of the poleward expansion of the Hadley cell edge and storm tracks on rainfall reductions since the 1970s over semiarid regions of the SH—namely, southern Australia and southern Africa during the austral autumn. These studies recognize that the changes in the circulation patterns have an impact on the long-term variability of rainfall. However, rainfall over extratropical latitudes is intimately related with synoptic-scale systems that are responsible for triggering individual rainfall events. Consequently, one should ask to what extent changes in the circulation patterns impact the preferred paths of the synoptic-scale systems that are the main triggering mechanisms for extratropical rainy events.

The passage of extratropical cyclones and anticyclones and their associated frontal systems play a major role in climate over mid- to high latitudes. They are responsible of the local weather and its variability and they represent the dynamical mechanisms that directly influence precipitation, temperature, cloudiness, radiation, and

geochemical tracers. They have a strong influence on the general circulation of the atmosphere owing to the horizontal moisture heat and momentum transport, and they interact with the low-frequency variability patterns of the atmospheric circulation such as the quasi-stationary waves triggered by remote forcings. Accordingly, any change in the characteristics of the frontal systems in terms of their intensity, frequency, or their characteristic pathways will certainly have an influence on the local climate. Consequently, the frontal activity may be used as a proxy for the dynamics of the extratropical lower troposphere strongly linked with cyclonic activity and storm tracks. Furthermore, the frontal activity is often associated with extreme rainfall events over subtropical and higher latitudes.

The connection between frontal activity and extratropical precipitation has been discussed in many studies, most of them focused on particular regions (e.g., Vera et al. 2002; Garreaud and Wallace 1998; Solman and Orlanski 2010). Recently, Catto et al. (2012) have quantified the amount of precipitation associated with fronts on a global basis and found that most of the 90% of the annual precipitation over the oceanic storm tracks in the SH is associated with the passage of frontal systems.

Given the importance of frontal systems on the occurrence of precipitation events over extratropical latitudes and their link with the dynamics of the troposphere, a measure of frontal activity (FA), introduced in Solman and Orlanski (2010), has been used in this study in order to evaluate the behavior of the frontal activity over the last 40 years and to explore the coherency of the change in FA during the late 1970s with the poleward shift of the westerly jet reported in earlier studies. Moreover, we also explore the consistency between the FA changes and the change in precipitation over subtropical and high latitudes of the SH. Though most of the studies focused on identifying consistent trends of rainfall during the last 50 years have been regionally focused, and the major precipitation changes have been identified over tropical regions, there is a general consensus on the increase of precipitation over high latitudes and decrease over mid-latitudes in the SH (Adler et al. 2008; Kang et al. 2011; Fyfe et al. 2012). We will show that some of the observed trends in rainfall over extratropical latitudes of the SH may be associated with changes in the frontal activity.

To summarize, in this paper we focus in two main questions: 1) The jet has moved poleward, at least during the warm season. Can we see that both the precipitation and fronts have the same displacement? 2) Can we find a correlation between frontal activity and the precipitation changes?

The frontal activity definition is based on two main features of frontal systems: a thermal contrast and the

associated cyclonic relative vorticity at 850 hPa. The datasets and methodology for computing the FA are described in section 2. Results are presented in section 3, in which the climatology of the FA is described and the change of the FA over the period 1962–2001 is explored. Furthermore, the extent to which the change in FA is coherent with the change in the extratropical circulation and precipitation is also discussed. Finally, conclusions and discussions are presented in section 4.

2. Methodology and data

The dataset used in this study to calculate the frontal activity and other circulation variables is from the 40-yr European Centre for Medium-Range Weather Forecasts (ECMWF) Re-Analysis (ERA-40; Uppala et al. 2005). The 40-yr period from 1962 to 2001 was used. ERA-40 data were available on a regular 2.5° grid. Marshall (2003) has examined the quality of this dataset and showed that it can be used with high confidence for examining the atmospheric circulation variability and recent trends of the high latitudes of the SH.

For the computation of the FA, the 1200 UTC fields of the meridional and zonal components of the wind and the temperature field at 850 hPa were used. The FA defined here captures the main properties of midlatitude frontal activity mainly associated with cold fronts: a thermal contrast and an associated cyclonic relative vorticity at lower levels of the troposphere, as in Solman and Orlanski (2010). Therefore, first, the zonal anomaly of the temperature and winds were calculated. Then, the absolute value of the gradient of the zonal anomaly of the temperature and the relative vorticity computed on the zonal anomalies of the meridional and zonal components of the wind were calculated. Then, the product between the temperature gradient and the relative vorticity ξ was computed. Cold fronts are associated with strong negative relative vorticity in the SH and strong horizontal temperature gradients; hence, the FA was multiplied by -1 in order to define positive values of the FA associated with cold fronts.

The FA diagnostic used in this study is motivated, in the first place, by the need to identify an objective measure for frontal systems detection. Though several studies leading with high-frequency synoptic-scale activity at extratropical latitudes are based on cyclonic vorticity centers (e.g., Hoskins and Hodges 2005; Field and Wood 2007) extratropical frontal systems are associated not only with cyclonic systems but also with an interface of air masses with different thermal characteristics. These two main features are included in the definition of FA. Moreover, synoptic charts allow for identifying several common characteristics associated

with the location of fronts, the location of the thermal gradients, and the associated cyclonic center, the frontal system being usually located over the region of the largest thermal contrast equatorward the maximum cyclonic vorticity center. Consequently, including the local thermal gradient in the FA definition has two purposes. First, the local thermal gradients are usually small over tropical regions, which prevents capturing cyclonic centers that are not related with frontal systems in the tropics. Second, it allows for locating the front shifted from the region of maximum cyclonic vorticity.

The FA diagnostic is also motivated by the strong link between fronts and precipitation. It is a well-known fact that extratropical precipitation is mostly forced convection and the major forcing is due to frontal systems. Moreover, many studies have recognized that several extreme rainfall events are associated with the passage of frontal systems. Details on the FA behavior for several selected cases can be found in the appendix.

The meridional component of the wind at various vertical levels in the troposphere (850, 700, 500, 400, and 300 hPa) was also used for exploring the vertical structure of the standard deviation of the meridional wind.

For the computation of the climatology of the FA, only cyclonic systems were considered (i.e., positive values of FA). The difference between the last 20 years of the dataset, from 1982 to 2001, and the first 20 years, from 1962 to 1981, is considered as a measure of climate change. Note that some interdecadal variability signals may be masked out by averaging over these two 20-yr periods. The analysis was performed for three extended seasons: SH summer [January–April (JFMA)], SH winter [May–August (MJJA)], and SH spring [September–December (SOND)].

Monthly precipitation data from the ERA-40 dataset was also used to explore the consistency between the changes in precipitation and the frontal activity during the 40-yr period analyzed. The choice of the ERA-40 precipitation dataset is made on the basis of its consistency with the circulation fields and the availability of an extended period with data covering both oceanic and land areas. However, other datasets of precipitation available with global coverage, such as the Global Precipitation Climatology Project (GPCP) (Adler et al. 2003) dataset and the Interim ECMWF Re-Analysis (ERA-Interim) (Dee et al. 2011) dataset were also used for the overlapping period from 1979 to 2001 in order to evaluate the consistency among different sources of precipitation data. Preliminary comparisons between the ERA-40 and the GPCP precipitation datasets have shown an overall good agreement mainly on the seasonal climatologies over subtropical and high latitudes of the SH. Moreover, Bosilovich et al. (2008) provide

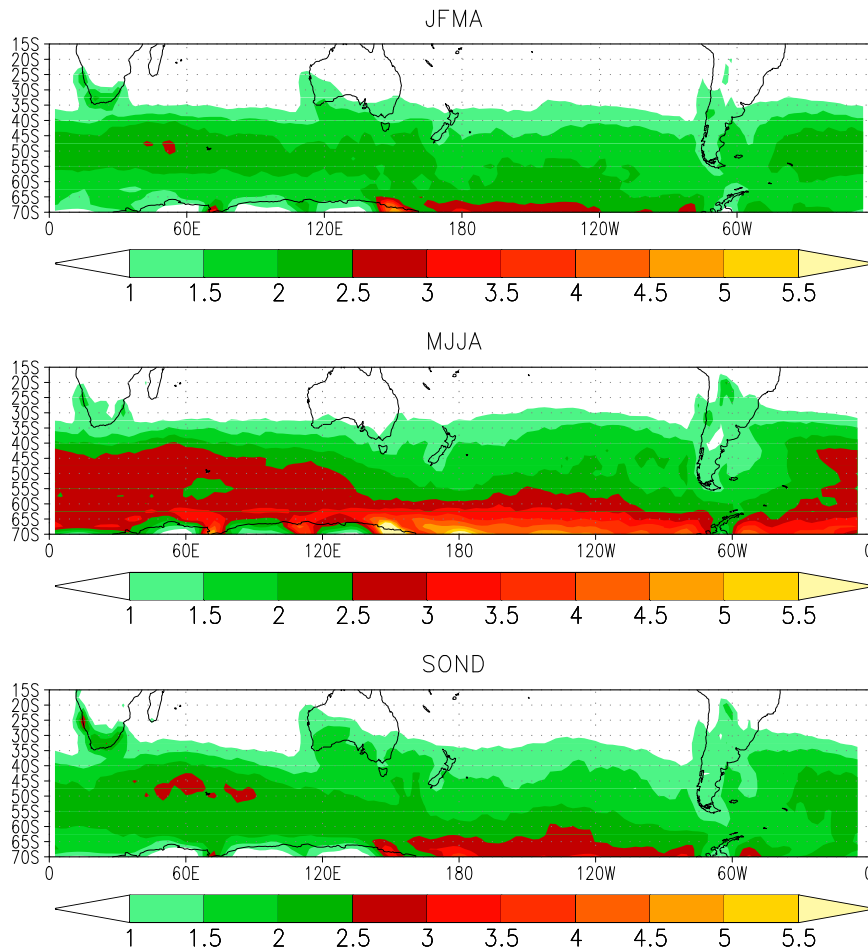


FIG. 1. Climatology of the frontal activity averaged for the period 1962–2001 for cyclonic systems only: (top) JFMA, (middle) MJJA, and (bottom) SON. Values larger than $1 \times 10^{-10} \text{C m}^{-1} \text{s}^{-1}$ are shaded.

some metrics on the evaluation of the quality of several monthly precipitation datasets from reanalysis and showed that the spatial correlation of the ERA-40 with GPCP over the high latitudes of the Southern Hemisphere is close to 0.9.

3. Results

a. Climatology of the frontal activity

The climatology of the FA introduced in this work is first analyzed in order to verify the behavior of this metric and its consistency with the well-known storm-track patterns of the SH. Figure 1 displays the climatology of the frontal activity averaged over the complete period of analysis (1962–2001) for the three extended seasons: JFMA, MJJA, and SON. This climatology has been computed for cyclonic systems only. Regions where the height of the topography is greater than 1.5 km were

masked out. Overall, the pattern of climatological FA is consistent with the pattern of bandpass filtered meridional wind and vorticity variance, which describes storm tracks that spiral in from midlatitudes into the circumpolar trough as shown, for example, in Hoskins and Hodges (2005, their Figs. 3c,d). Moreover, the seasonal variation of the FA also agrees with the seasonal variation of the SH storm tracks discussed elsewhere. In particular, during the SH winter (MJJA), the FA attains larger intensity and is extended over a broader range of latitudes, which is consistent with the seasonal migration of the SH storm track. There are also large values of FA in all seasons over the periphery of Antarctica, which may be due to strong thermal contrasts and hence baroclinicity over the sea ice edge. Note that the larger intensity and frequency of the cyclonic activity during the SH winter over Australia and South Africa is particularly evident at upper levels but not at lower levels, which is in agreement with Hoskins and Hodges (2005).

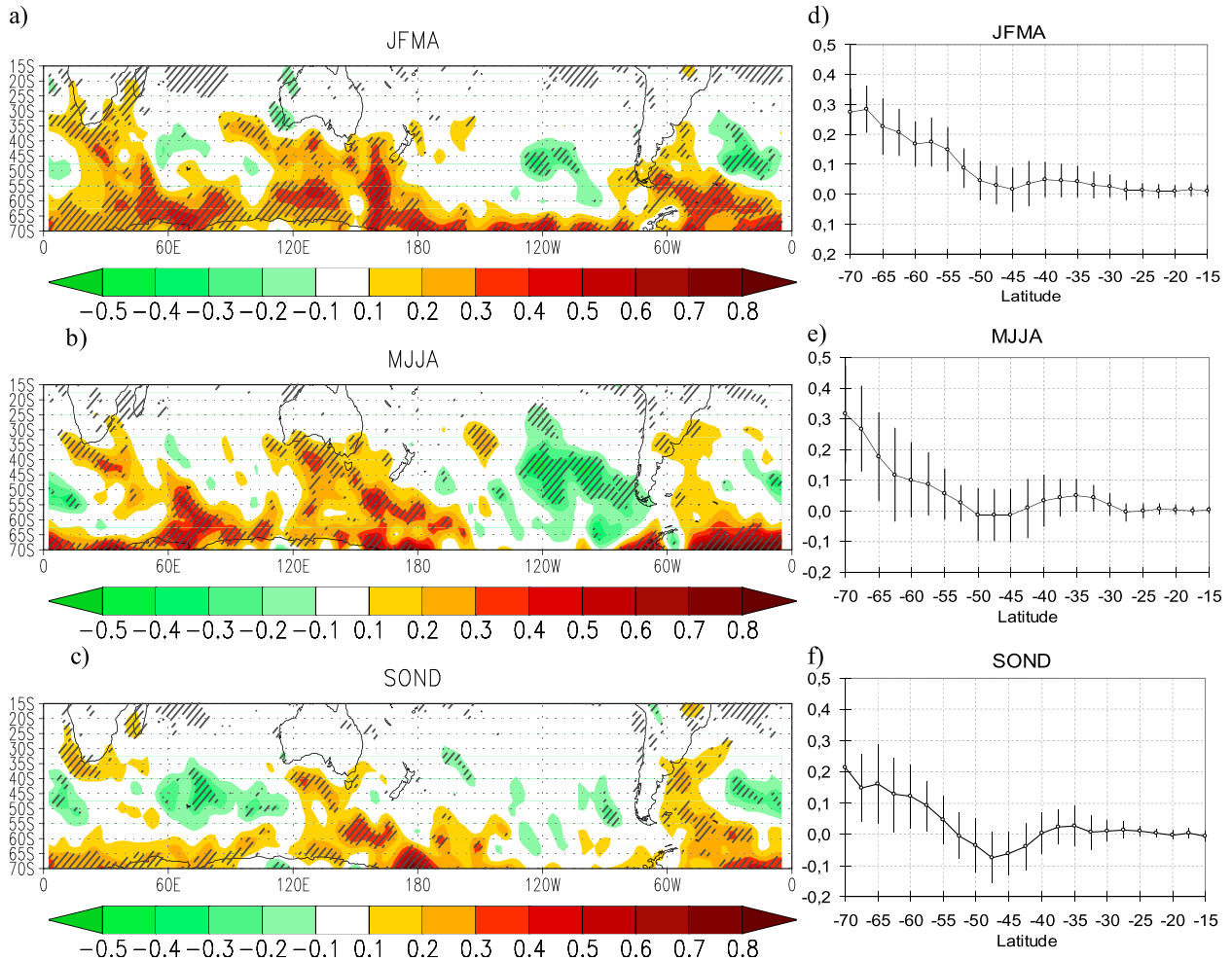


FIG. 2. Differences between 1982–2001 and 1962–81 for the frontal activity (cyclonic systems only): (a) JFMA, (b) MJJA, and (c) SOND. Hatched areas indicate where the differences in FA are statistically significant at the 95% level. (d)–(f) Zonally averaged differences of FA. Vertical bars indicate plus or minus one standard deviation calculated from monthly values. Units are $^{\circ}\text{C m}^{-1} \text{s}^{-1} \times 10^{-10}$.

It is important to remark that not all the frontal systems are associated with rainfall events. Although the frontal activity is larger (smaller) during the warm (cold) season, over some particular regions such as southern Africa and Australia, the frequency of fronts with no precipitation is close to 80% (10%–50%). The climatology of frontal activity discussed here agrees broadly with the results shown by Berry et al. (2011), who performed a climatology of atmospheric fronts based on the ERA-40, although their definition of fronts was based on the gradient of the wet-bulb potential temperature at 850 hPa.

b. Changes in FA

Recent studies have shown that the poleward shift of the SH storm tracks during the last decades can be identified by means of different metrics accounting for synoptic-scale activity such as cyclone density (Wang

et al. 2006), storm cloudiness (Bender et al. 2012), and cyclone-tracking techniques (Frederiksen and Frederiksen 2007). Frontal systems are intimately linked with the storm tracks, being the near-surface manifestation of the synoptic-scale activity. Consequently, we explore in this section to what extent the frontal activity changes during the last decades are consistent with the changes in storm tracks and with the poleward shift of the westerly jet, reported in previous studies.

The difference of the FA between the climatic mean for the period 1982–2001 and the period 1962–81 is shown in Fig. 2 for JFMA, MJJA, and SOND. A robust climate signal is found where the differences are significant at the 95% level using a two-tailed Student's *t* test. The frontal activity over high latitudes of the SH (around 60°S) has increased significantly in all seasons, although the largest changes are more extensive during the SH summer and

winter seasons. A poleward shift of FA is clearly seen mainly during JFMA and SOND, with increasing FA at high latitudes and decreasing FA at subtropical latitudes. However, the change of FA is not zonally symmetric, but three regions with larger changes can be identified: southern Indian Ocean, southern Australia, and the southeastern Pacific–southeastern South America sector. During MJJA the change of FA also shows a significant decrease over the eastern sector of the Pacific Ocean. The changes in storminess (vorticity) and baroclinicity (thermal gradient) as well as the changes in their variances (not shown) suggest that the contributions of the two parameters are important in explaining the FA change. Regions with the largest FA increases (decreases) are regions where both storminess and baroclinicity and their variances increase (decrease). However, there are some particular regions (such as the Indian Ocean during SOND) where changes in vorticity dominate. Moreover, there are regions where the increase in the vorticity variance is compensated by a decrease in the thermal gradient variance, though the former has a dominant contribution.

Figure 2 also shows the zonally averaged change of the FA. A large increase of the FA at high latitudes of the SH all year round is apparent, suggesting a poleward expansion of the regions with larger frontal activity. During JFMA a poleward shift of the latitude of maximum frontal activity, around 55°S, is masked out by the large increase of FA at all latitudes (not shown). During MJJA and SOND, Fig. 2 suggests an expansion and poleward shift of the region of maximum frontal activity identified in Fig. 1 with a slight decrease of frontal activity over the 40°–50°S latitude band. These results agree with Wang et al. (2006), who evaluated trends in cyclone activity over the SH and found an increasing trend of strong-cyclone activity over the austral circumpolar oceanic region with a decreasing trend over the 40°–60°S zone over the southeastern Pacific Ocean during the austral winter season. However, owing to the asymmetries in the pattern of the FA change, the zonal mean changes are small owing to compensating areas with FA increase and areas with FA decrease.

Figure 3 shows the difference of the 300-hPa geopotential height zonal anomalies superimposed to the FA difference. During JFMA and MJJA, the climatic change of the zonal anomalies of the 300-hPa height field is characterized by a Rossby wave pattern emanating from the Indian Ocean and propagating throughout the Pacific Ocean, with a zonal wavenumber-3 structure, resembling the well-known Pacific–South American (PSA) pattern (Mo and Paegle 2001). The zonally asymmetric climatic change signal is characterized by two strong positive anomalies located over the Indian Ocean and the southeastern Pacific Ocean. This pattern of change of

the 300-hPa zonal anomalies may be associated with the larger number of El Niño events during the last 20 years of the period analyzed, which is in agreement with Hobbs and Raphael (2007). Moreover, the pattern of change in the zonal anomaly field agrees with the poleward and eastward shift of the Pacific ridge (Hobbs and Raphael 2007).

During the spring season, the climatic change of the zonal anomalies at 300 hPa presents a wavenumber-1 structure with increasing (decreasing) anomalies over the Indian and Atlantic Oceans (Pacific Ocean), suggesting a poleward and eastward shift of the zonal wavenumber-1 structure (Raphael 2003). This pattern of change indicates a weakening of the southeastern Pacific anticyclone and the Indian Ocean trough.

For all seasons, there is an overall consistency between the pattern of FA change and the change of the asymmetric component of the 300-hPa geopotential height. The positive (negative) anomalies of the FA are located upstream (downstream) the positive anomalies of the zonally asymmetric circulation, inducing a poleward shift of the frontal activity, indicating a clear link between the zonal asymmetries in the pattern of FA change with the asymmetric circulation.

c. Changes in frontal activity and storm tracks

Frontal systems are a manifestation of the high-frequency activity of the troposphere, usually referred to as storm tracks, which may be characterized by the standard deviation of the eddy meridional wind [Vera (2003) and references therein]. To evaluate the consistency between changes in frontal activity and changes in the midlatitude storm tracks, the vertical structure of the change of the zonally averaged storm tracks is displayed in Fig. 4, together with its climatology. A robust climate signal is found where the differences are significant at the 95% level using two-tailed *F* test.

It is a well-known fact that the storm tracks attain their largest intensity at the upper levels in the troposphere, with a rapid decrease in amplitude downward, with the largest eddy activity at lower levels slightly poleward with respect to upper levels. Note that latitudes with larger storm-track amplitude at lower levels agree with regions with larger FA shown in Fig. 1. The change in storm track clearly indicates the poleward expansion of storm track all year long, with the largest changes during the austral summer. The major increase in the amplitude of the storm tracks at high latitudes (around 60°S) agrees with the increase of frontal activity shown in Fig. 2, being the largest changes in both storm track and frontal activity during the austral summer. Note also that during MJJA a slight increase of the amplitude of the eddy activity is apparent at the subtropical branch of the storm track in

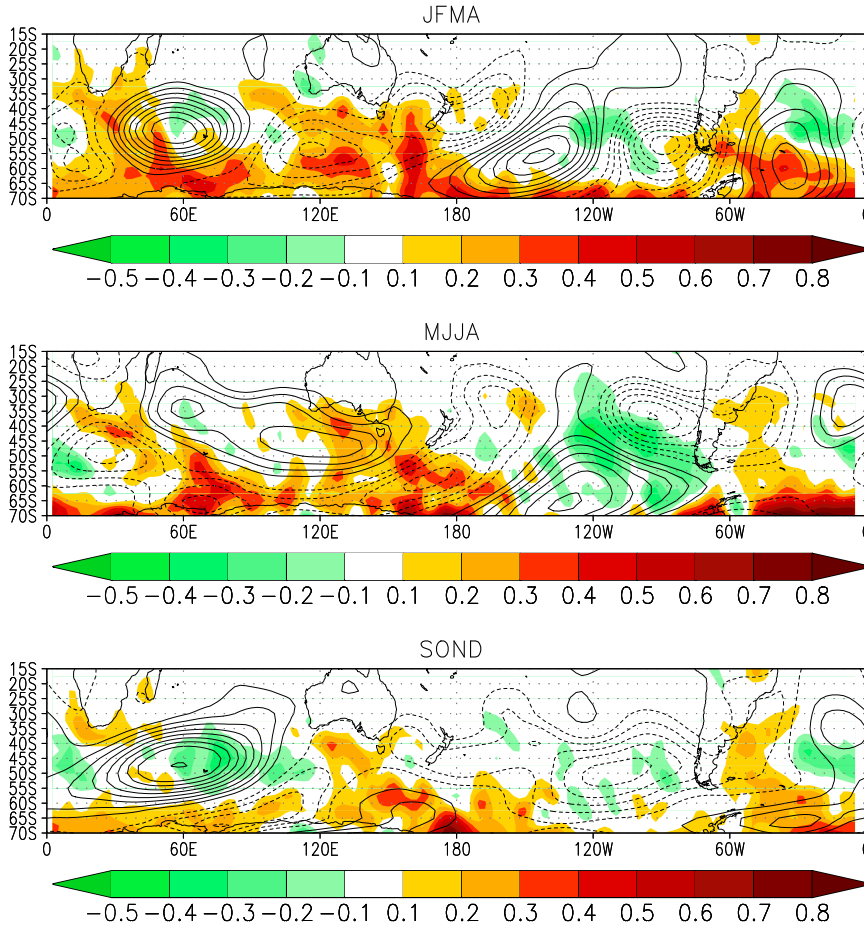


FIG. 3. Differences between 1982–2001 and 1962–81 for the frontal activity (cyclonic systems only) (shaded; $^{\circ}\text{C m}^{-1} \text{s}^{-1} \times 10^{-10}$) and for the zonal anomaly of the 300-hPa geopotential height (Z300, contour interval 50 m; zero contours omitted): (top) JFMA, (middle) MJJA, and (bottom) SOND.

the upper troposphere, which is consistent with the FA increase at the subtropical band shown in Fig. 2e. The changes in the storm track are, however, characterized by strong zonal asymmetries. Inspection of the differences of the storm tracks at 850 hPa (not shown) reveals a strong consistency with the changes in frontal activity, with a large area of weakening over the subtropical Pacific Ocean during the three seasons analyzed.

Overall, a clear consistency between the changes in the frontal activity and storm tracks takes place, as expected, with the largest changes occurring during the austral summer months characterized by a poleward expansion of the storm tracks, which is in agreement with a poleward expansion of the areas with larger frontal activity.

d. Changes in frontal activity and precipitation

The relationship between precipitation and fronts has been discussed by several authors. The percentage of rainfall associated with fronts has been found to be

around 70%–80% at extratropical latitudes of the SH during all seasons (not shown), which is in agreement with Catto et al. (2012). Hence, owing to the close relationship between rainfall events and frontal systems, it is expected that changes in the frontal activity may induce changes in rainfall. Figure 5 shows the normalized difference of precipitation from the ERA-40 dataset between 1982–2001 and 1962–81. The significance of the difference in precipitation has been tested using a two-tailed Student’s *t* test at the 95% level. Although some caveats on the quality of the precipitation reanalysis products should be considered (Bosilovich et al. 2008), particularly over the high latitudes of the SH before the satellite era, this analysis allows evaluating the consistency between the changes in the frontal activity and precipitation from the same reanalysis dataset.

The most remarkable features of the normalized change in precipitation from the ERA-40 dataset are a decrease over the central Pacific, Atlantic, and Indian

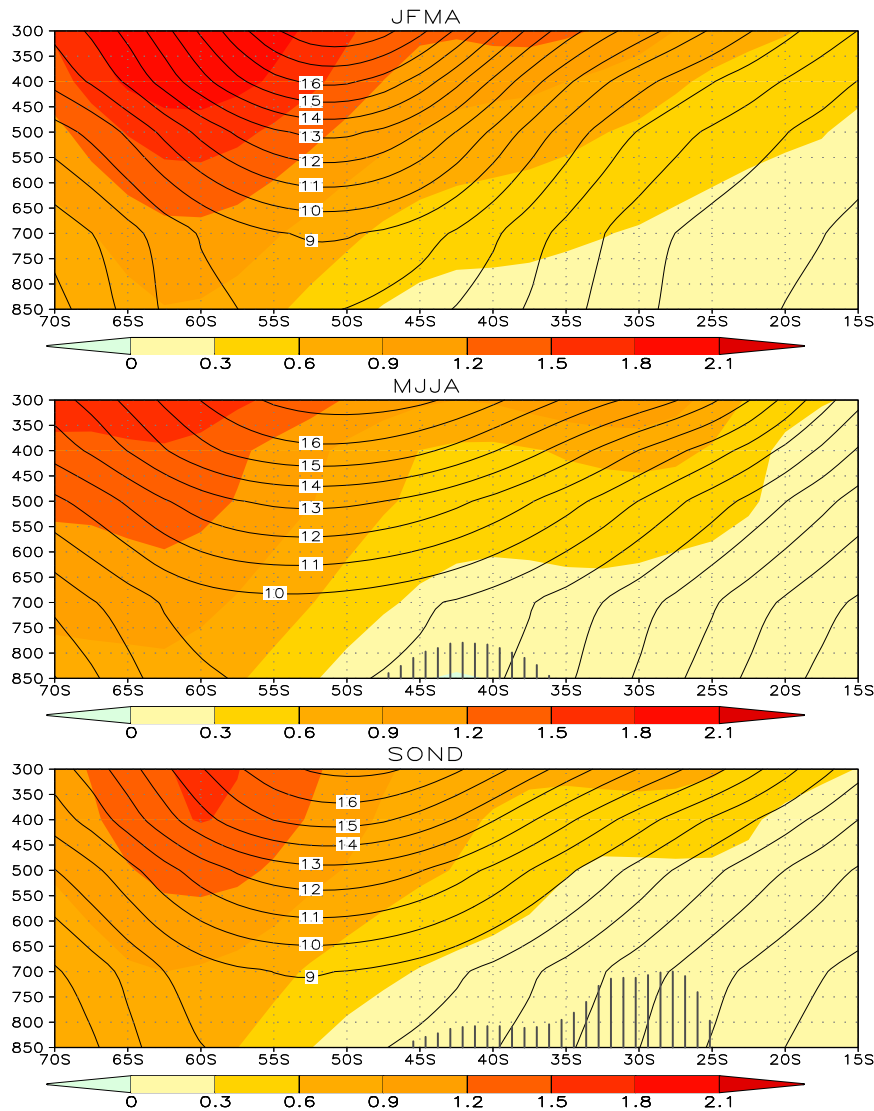


FIG. 4. Climatology of the vertical profile of the zonally averaged standard deviation of the meridional component of the wind for the 1962–2001 period (contours; m s^{-1}) and its difference between 1982–2001 and 1962–81 (shaded; m s^{-1}). Hatched areas denote where the differences in the standard deviation are not significant at the 95% level.

Oceans between 35° and 50°S and an increase at subpolar latitudes in all seasons. This pattern of change suggests a midlatitude drying and high-latitude moistening and hence a poleward shift of the regions with large precipitation at the extratropical SH, which is in agreement with Fyfe et al. (2012), Kang et al. (2011), and Purich et al. (2013). Note also the precipitation increase over central South America during JFMA, which is in agreement with observational studies (Liebmann et al. 2004). During MJJA, enhanced drying conditions are seen across the midlatitudes with a large precipitation decrease over the central and eastern South Pacific Ocean extending over the southwestern coast of South America

(with anomalies exceeding one standard deviation) and rainfall increases over central South America. The precipitation change over southeastern Australia and southern Africa suggests wetter conditions, which is not consistent with studies of rainfall trends over those regions (Taschetto and England 2009; Cai et al. 2012; Purich et al. 2013). The rainfall trend calculated for the period 1982–2001 from the ERA-40 dataset was compared with results from the GPCP dataset (not shown) and it was found that for the last 20 years, the ERA-40 agrees well with observations. The poor quality of the ERA-40 precipitation data during the first 20 years included in the analysis may explain this inconsistency.

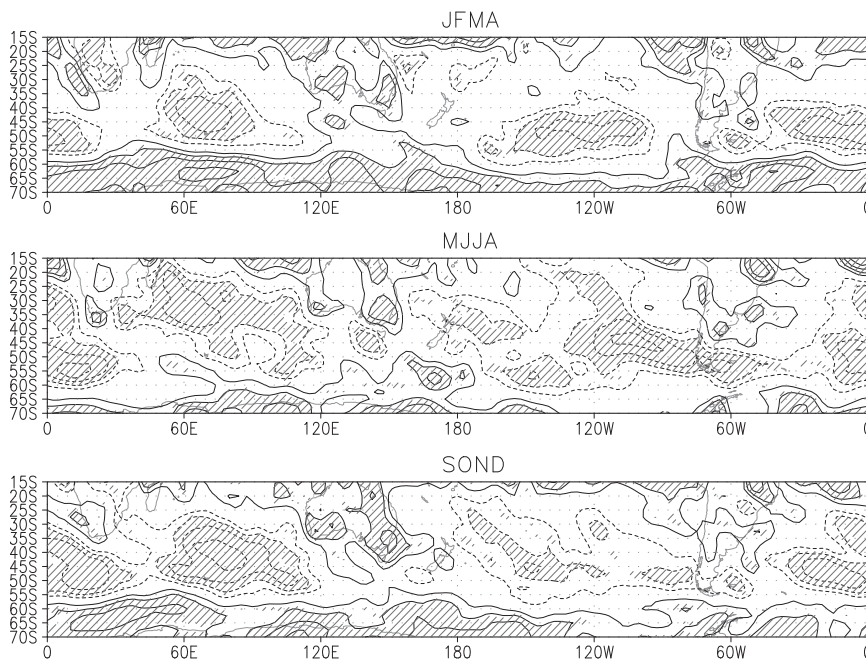


FIG. 5. As in Fig. 3, but for the normalized difference of precipitation [contours interval 0.2 (unitless); zero contours omitted.]. Hatched areas indicate where the differences in precipitation are statistically significant at the 95% level.

During SON, the largest precipitation decrease occurs over the central Indian Ocean basin. Significant rainfall increase is also apparent over continental areas at the subtropics, which is in agreement with observational studies.

Figure 6 displays the normalized precipitation change together with the normalized FA change. The most outstanding feature is that the pattern of precipitation change is consistent with the pattern of frontal activity change, suggesting that the drying (moistening) conditions over midlatitudes (subpolar latitudes) of the SH may be associated with the decrease (increase) of the frontal activity over midlatitudes (subpolar latitudes). Note also that the zonal asymmetry in the pattern of precipitation changes also agrees with the zonal asymmetries in the pattern of frontal activity changes. Moreover, the regions with the largest FA changes agree with the regions of the largest precipitation changes, indicating a strong relationship between the climatic change signal of rainfall and frontal activity. However, this consistency is not apparent for some specific regions (such as south of Australia during MJJA).

The climatic change signal discussed so far is based on the differences between two periods, before and after the 1980s (1962–81 and 1982–2001), and a robust consistency was found between changes in precipitation and frontal activity. Overall, it was shown that the midlatitudes and subpolar regions seem to show opposite behavior in terms

of precipitation and frontal activity changes, suggesting a poleward shift in frontal activity associated with the midlatitudes drying and high latitudes wetting. However, the atmospheric circulation patterns and precipitation are characterized by large variations from year to year and from decade to decade [see Pezza et al. (2007), Garreaud and Battisti (1999), and references therein] and the climatic differences analyzed may mask signals of low-frequency variability. Consequently, a closer inspection of the consistency between frontal activity and precipitation variability has been done by analyzing the temporal evolution of the normalized monthly anomalies zonally averaged over two latitudinal bands: one at midlatitudes (from 50° to 30°S) and another at high latitudes (from 70° to 50°S). The difference between the normalized anomalies averaged over the high-latitude band and the midlatitude band for both precipitation and frontal activity are shown in Fig. 7. In addition, and in order to verify the temporal evolution of the precipitation anomalies from the ERA-40 dataset, monthly precipitation data from GPCP and ERA-Interim for the period 1979–2001 have also been included. This analysis allows for verifying the consistency between frontal activity and precipitation on shorter time scales (from interannual to interdecadal) but also for verifying if this consistency arises for an independent source of data.

For every season, Fig. 7 suggests a closed consistency between the temporal evolution of the difference between

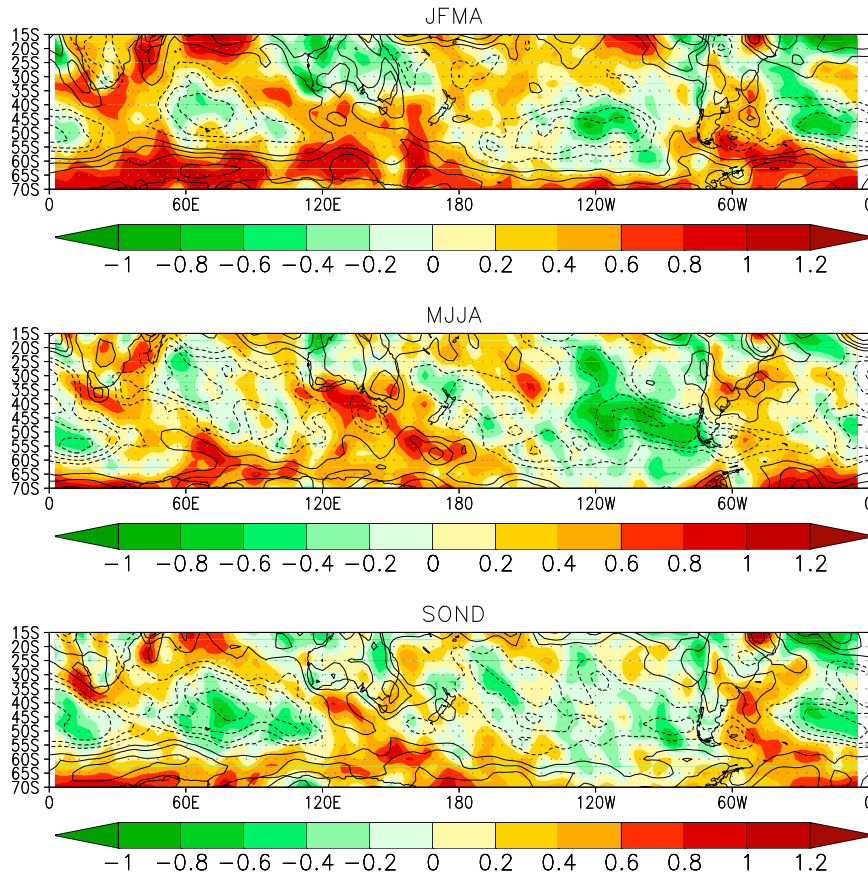


FIG. 6. As in Fig. 3, but for the normalized difference of precipitation [contour interval 0.2 (unitless); zero contours omitted] superimposed on the normalized difference of FA (shaded; unitless).

high and midlatitudes of the precipitation and frontal activity anomalies from year to year. Throughout the period of analysis, peaks of anomalous precipitation have a strong correspondence with peaks of anomalous frontal activity. The linear correlation coefficients calculated between the FA time series and the time series from the various precipitation datasets (shown in Fig. 7) confirm the close relationship between the two variables. This consistency is also verified for anomalies at both high and midlatitudes (not shown).

During JFMA, a significant positive trend of $0.46 \pm 0.01 \text{ decade}^{-1}$ for the normalized frontal activity difference and a significant positive trend of $0.63 \pm 0.01 \text{ decade}^{-1}$ for the normalized precipitation difference (using 95% confidence intervals) were found. Moreover, the portion of the precipitation trend that is congruent with the FA trend, computed by multiplying the regression coefficient by the FA trend and dividing by the precipitation trend is 64%, suggesting the strong control exerted by the frontal activity on precipitation. However, the positive trends are significant only for both

frontal activity and precipitation at the high-latitude band, suggesting that moistening at high latitudes is strongly associated with the increase in the frontal activity owing to the poleward expansion of the storm track during the austral summer months. At midlatitudes, neither the frontal activity nor precipitation show significant trends over the 1962–2001 period. The temporal evolution of the precipitation anomalies from ERA-40, ERA-Interim, and GPCP for the period 1979–2001 suggests that an overall agreement is apparent; however, rainfall from ERA-40 shows strong discrepancies compared with GPCP. Moreover, ERA-Interim seems to agree better with GPCP than compared with the ERA-40 dataset. However, the consistency between frontal activity and precipitation is also apparent. For the period 1979–2001, the difference of frontal activity between high and midlatitudes yields a trend of $0.5 \pm 0.02 \text{ decade}^{-1}$, the GPCP precipitation dataset yields a trend of $0.8 \pm 0.05 \text{ decade}^{-1}$, and the ERA-Interim precipitation dataset yields a trend of $0.9 \pm 0.4 \text{ decade}^{-1}$. In all cases the trends are significant at the 95% confidence level. The corresponding

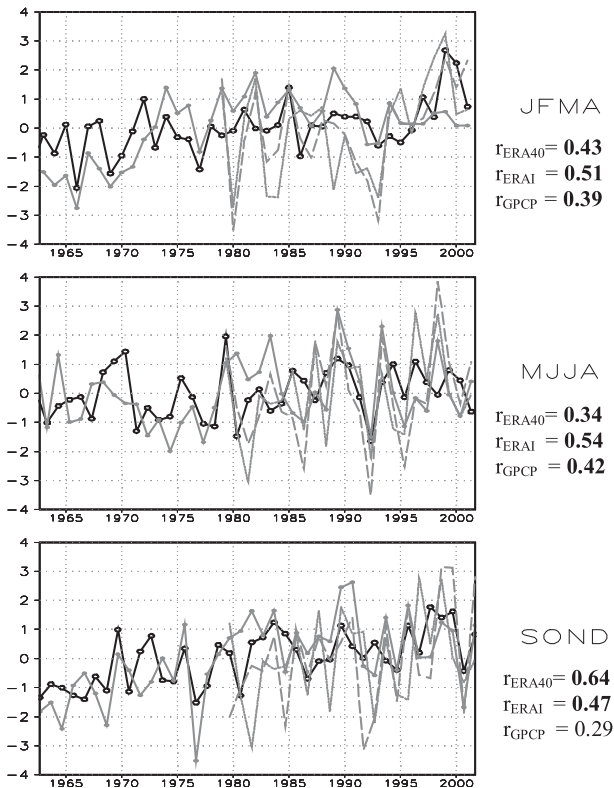


FIG. 7. Time series of the difference of the zonal mean anomalies averaged over subpolar latitudes (70° – 50° S) and over subtropical latitudes (50° – 30° S) of frontal activity (black lines) and precipitation (gray lines) normalized by their respective standard deviations. Seasonal means for (top) JFMA, (middle) MJJA, and (bottom) SON. Solid, dotted, and dashed lines correspond to ERA-40, GPCP, and ERA-Interim precipitation data, respectively. The correlation coefficients between the FA time series and the corresponding precipitation time series are indicated beside each panel. Significant correlations (at the 95% level) are indicated in boldface.

percentages of precipitation trends due to the FA trend are 49% and 54%, respectively. The precipitation trends discussed here agree with Fyfe et al. (2012), who showed consistent trends in sea level pressure and related poleward-shifting surface westerlies and extratropical storm track as drivers of the rainfall trends observed during recent decades. What is new in our findings is that the changes in the frontal activity—strongly connected with the changes in the atmospheric circulation—account for a large proportion of the precipitation changes.

During MJJA, the difference between high and mid-latitudes of the zonally averaged normalized anomalies of precipitation and frontal activity do not display significant trends. Moreover, no significant trends are found for the high and midlatitudes. It is important to bear in mind that the zonal symmetry of the precipitation change is more evident during JFMA and SON, but during MJJA large asymmetries are apparent, strongly associated

with the asymmetric component of the climate change signal, as discussed in previous sections.

The behavior during SON is similar to that during JFMA, but with a significant increase (decrease) of the frontal activity and precipitation at high (mid-) latitudes throughout the 1962–2001 period, summarized in significant positive trends of the difference shown in Fig. 7. However, the trends are much weaker when evaluating over the 1979–2001 period. The percentage of the precipitation trend from the ERA-40 dataset attributed to the FA trend is 74% for the 1962–2001 period. In comparison, the portion of the precipitation trend from GPCP and ERA-Interim due to FA is 40%.

Overall, results displayed in Fig. 7 highlight the strong correspondence between frontal activity and precipitation, not only in terms of the trends over the last 40 years, but also in terms of the variability. Moreover, it was shown that a large amount (more than 50%) of the zonal mean precipitation trends is congruent with the FA trend during both JFMA and SON. This is a robust result that suggests that understanding the mechanisms leading to the frontal activity changes will certainly help to understand the patterns of precipitation change.

4. Summary and conclusions

The focus of the research presented here is to explore the consistency between the poleward shift in the midlatitude westerlies and storm tracks during the last decades of the twentieth century in the SH, reported in previous studies, with the poleward shift of frontal activity. Moreover, the analysis also allowed for exploring the correlation between fronts and precipitation, suggesting that the changes in precipitation are strongly tied to changes in frontal activity at the subtropical and subpolar latitudes of the SH.

Frontal activity, a proxy for the dynamics of the lower troposphere, is defined in terms of the temperature gradient times the relative vorticity, the main features associated with the passage of midlatitude fronts, using the ERA-40 dataset during the period from 1962 to 2001. The climatology of frontal activity associated with cyclonic systems revealed that this measure captures the main features of the synoptic-scale activity at subtropical and high latitudes of the SH along the year, as compared with other studies based on other measures of synoptic activity and frontal systems (Hosking and Hodges 2005; Berry et al. 2011).

The climatic change of the frontal activity, calculated as the difference between two 20-yr periods (1962–81 and 1982–2001) shows a considerable increase at high latitudes of the SH and a decrease at subtropical latitudes, mainly during the austral summer and spring months. This poleward shift in frontal activity is consistent with reported changes of the zonal wind at both

upper and lower levels in the troposphere (e.g., Archer and Caldeira 2008) and also consistent with the poleward expansion of the storm tracks. However, the change in frontal activity is not zonally symmetric, with the zonal asymmetries consistent with the climate change signal of the zonal anomaly of the 300-hPa geopotential height for all seasons. Regions with increased (decreased) frontal activity are located upstream (downstream) of positive (negative) changes in the zonally asymmetric component of the upper-tropospheric circulation. The more remarkable features of the zonally asymmetric climate change signal in the SH troposphere are two quasi-stationary anticyclones located south of the Indian Ocean and the eastern Pacific during both summer and winter months, which may inhibit the passage of frontal systems. These anomalous anticyclones may be associated with increasing blocking episodes that may affect the trajectory of the traveling cyclonic systems and, consequently, suppress the frontal activity.

Precipitation changes also show a consistent poleward shift mainly during the austral summer and spring seasons, which is in agreement with other studies, such as Fyfe et al. (2012) and references therein. This pattern of precipitation change is consistent with the poleward shift in the westerlies, the storm tracks, and the frontal activity. Moreover, a close correspondence is found between frontal activity and precipitation, both in terms of the spatial pattern of the changes and the temporal evolution of anomalies at high and midlatitudes of the SH. It is shown that regions with a significant increase (decrease) in frontal activity also show a significant increase (decrease) in precipitation, suggesting that precipitation changes are strongly controlled by the changes in frontal activity at mid- and subpolar latitudes. This close correspondence is also present when exploring the year-to-year variability of both precipitation and frontal activity anomalies at mid- and high latitudes: years with peak positive precipitation anomalies also show peak positive frontal activity anomalies. Moreover, it was demonstrated that at least a 50% of the zonal mean precipitation trends is congruent with the FA trend during both JFMA and SOND. However, the frontal activity has a complex relationship with rainfall owing to the fact that not every frontal system is associated with rainfall events; consequently, the consistency between frontal activity and rainfall changes is not apparent over some specific regions.

These results emphasize a robust link between the change in the asymmetric component of the upper-level large-scale circulation, the change in the frontal activity, and the change in precipitation, which may help understanding future climate change projections.

Moreover, owing to the close relationship between precipitation and fronts, several questions arise, such as to what extent the reported and projected changes in

extreme precipitation events over southern South America, Australia, and Africa (Seneviratne et al. 2012) may be associated with the frontal activity behavior. Furthermore, we can also try to understand the dynamical mechanisms leading to the low-frequency variability patterns of precipitation discussed in the literature, exploring how the low-frequency variability patterns of the atmospheric circulation impact the frontal activity and, therefore, on precipitation.

Acknowledgments. The research leading to these results has received funding from the CONICET Grants PIP 112-200801-00195 and PIP 112-201101-00189 and UBACyT Grant Y028. This report was prepared under Award NA08OAR4320752 from the National Atmospheric and Oceanic Administration. The statements, findings, conclusions, and recommendations are those of the author(s) and do not necessarily reflect the views of the National Oceanic and Atmospheric Administration or the U.S. Department of Commerce. ERA-40 and ERA-Interim data have been provided by the European Centre for Medium-Range Weather Forecasts from their website at http://data-portal.ecmwf.int/data/d/era40_daily/ and at http://data-portal.ecmwf.int/data/d/interim_daily/, respectively. GPCP precipitation data provided by the NOAA/OAR/ESRL PSD, Boulder, Colorado, has been downloaded from their website at <http://www.esrl.noaa.gov/psd/>. The authors also thank two anonymous reviewers whose comments greatly helped to improve the manuscript.

APPENDIX

On the FA Index

In the following section, the motivation of the FA diagnostic is discussed. As stated in section 2, frontal systems at the extratropics are usually associated with both a cyclonic vorticity center and a local thermal contrast. Taking the product between these two measures allows for inclusion of these two criteria on the objective fronts generated by means of the FA index. Moreover, the extratropical frontal systems are usually associated with consistent rainfall patterns, owing to the control exerted by the frontal forcing on triggering convection at extratropical latitudes. The selected cases displayed in Fig. A1 show the FA capability in capturing the main features of frontal systems and associated precipitation compared against the infrared satellite imagery from the National Oceanic and Atmospheric Administration (NOAA) (downloaded from <ftp://eclipse.ncdc.noaa.gov/pub/gridsat/b1-climate-data-record/>) for three frontal systems that developed on 8 July 2000, 3 July 2001, and 23 June 1983.

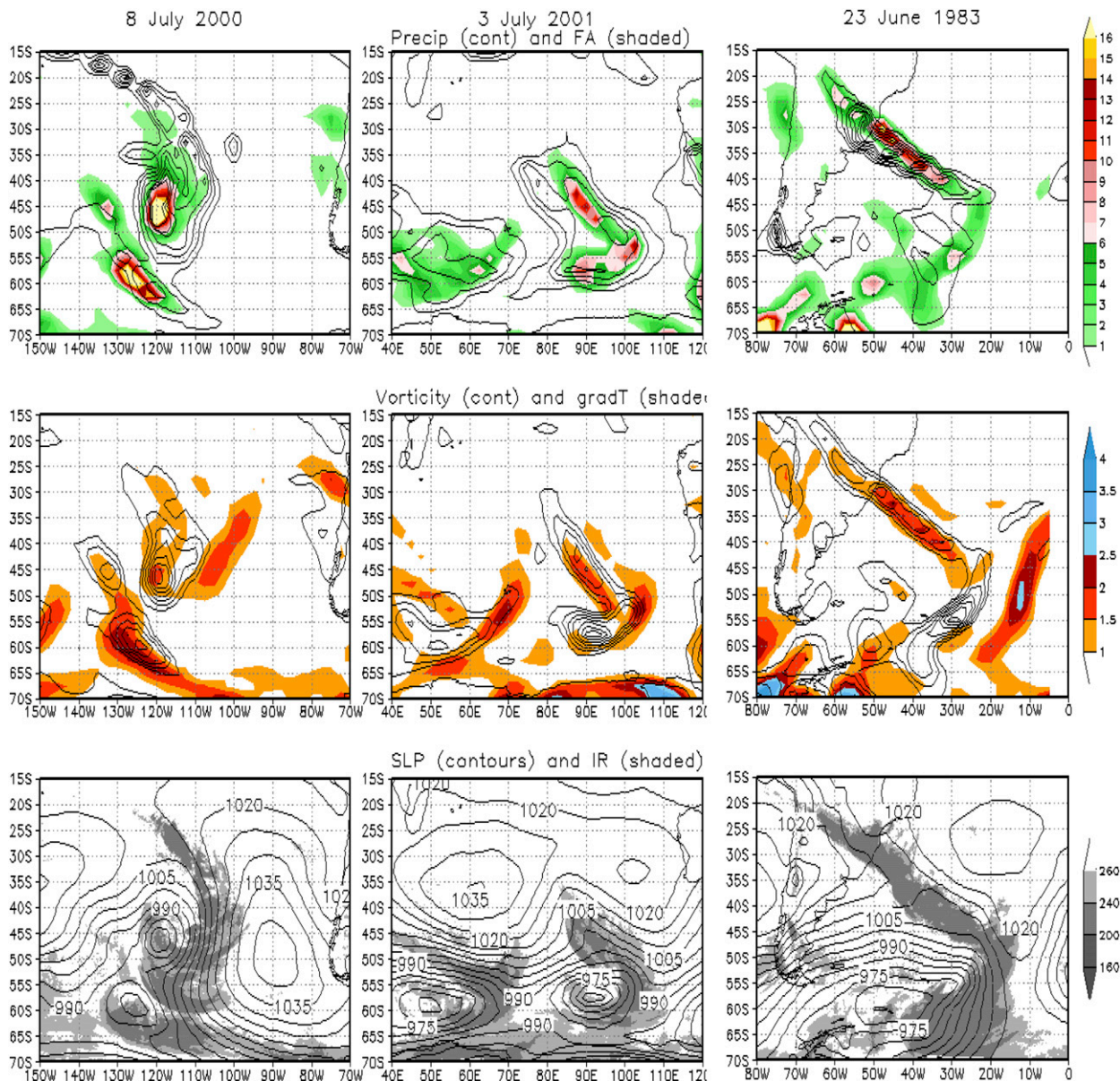


FIG. A1. Examples of the frontal features for (left) 8 Jul 2000, (center) 3 Jul 2001, and (right) 23 Jun 1983 events. (top) FA (shaded; $^{\circ}\text{C m}^{-1} \text{s}^{-1} \times 10^{-10}$) and associated precipitation [contours intervals (left) 4, (center) 2, and (right) 5 mm]. (middle) Cyclonic vorticity (contour interval $1 \times 10^5 \text{s}^{-1}$) and local thermal gradient (shaded; $10^{\circ}\text{C m}^{-1}$). (bottom) Infrared satellite imagery from NOAA (brightness temperature; shaded; K) and sea level pressure (contour interval 5 hPa).

For the first case, the infrared satellite imagery shows a well-defined frontal cloud band associated with a deep cyclonic system in a mature stage over the southwestern Pacific Ocean (around 45°S , 120°W). The front is aligned with the cloud band and the region with the largest thermal gradient; it lies downstream of the cyclone at surface and the corresponding center of maximum cyclonic vorticity and the associated precipitation is mostly equatorward the frontal system, as expected. For the second case, two frontal cloud bands can be identified from the infrared

satellite imagery over the central Indian Ocean at 55°S , 50°E and 55°S , 90°E . The FA captures the main features of these systems, but in these cases the associated rainfall is located over the frontal system. The FA maximum is shifted from the center of maximum cyclonic vorticity toward the region where the thermal gradients are larger. Finally, in the third case, a mature-stage cyclone over the southeastern Atlantic Ocean associated with an extended frontal cloud band is also captured by the FA. Note that the maximum FA intensity is located over the region

where both the thermal gradient and the cyclonic vorticity center are both relevant features.

An analysis over an extended area including tropical regions (not shown) suggests that including the local thermal gradient in the calculation of the FA has two purposes. First, it prevents capturing cyclonic vorticity centers not associated with frontal systems, owing to the fact that the thermal gradient is quite small over tropical latitudes. Second, it allows locating the frontal system aligned with the associated rainfall band and shifted from the center of maximum vorticity.

REFERENCES

- Adler, R. F., and Coauthors, 2003: The Version-2 Global Precipitation Climatology Project (GPCP) Monthly Precipitation Analysis (1979–present). *J. Hydrometeorol.*, **4**, 1147–1167.
- , G. Gu, J.-J. Wang, G. J. Huffman, S. Curtis, and D. Bolvin, 2008: Relationships between global precipitation and surface temperature on interannual and longer timescales (1979–2006). *J. Geophys. Res.*, **113**, D22104, doi:10.1029/2008JD010536.
- Archer, C. L., and K. Caldeira, 2008: Historical trends in the jet streams. *Geophys. Res. Lett.*, **35**, L08803, doi:10.1029/2008GL033614.
- Bender, F. A.-M., V. Ramanathan, and G. Tselioudis, 2012: Changes in extratropical storm track cloudiness 1983–2008: Observational support for a poleward shift. *Climate Dyn.*, **38**, 2937–2053.
- Berry, G. J., M. J. Reeder, and C. Jakob, 2011: A global climatology of atmospheric fronts. *Geophys. Res. Lett.*, **38**, L04809, doi:10.1029/2010GL046451.
- Bosilovich, M. G., J. Chen, F. R. Robertson, and R. F. Adler, 2008: Evaluation of global precipitation in reanalyses. *J. Appl. Meteor. Climatol.*, **47**, 2279–2299.
- Cai, W., T. Cowan, and M. Thatcher, 2012: Rainfall reductions over Southern Hemisphere semi-arid regions: The role of subtropical dry zone expansion. *Sci Rep*, **2**, 702, doi:10.1038/srep00702.
- Catto, J. L., C. Jakob, G. Berry, and N. Nicholls, 2012: Relating global precipitation to atmospheric fronts. *Geophys. Res. Lett.*, **39**, L10805, doi:10.1029/2012GL051736.
- Chen, G., and I. M. Held, 2007: Phase speed spectra and the recent poleward shift of Southern Hemisphere surface westerlies. *Geophys. Res. Lett.*, **34**, L21805, doi:10.1029/2007GL031200.
- Dee, D. P., and Coauthors, 2011: The ERA-Interim reanalysis: Configuration and performance of the data assimilation system. *Quart. J. Roy. Meteor. Soc.*, **137**, 553–597, doi:10.1002/qj.828.
- Field, P. R., and R. Wood, 2007: Precipitation and cloud structure in midlatitude cyclones. *J. Climate*, **20**, 233–254.
- Frederiksen, J., and C. Frederiksen, 2007: Interdecadal changes in southern hemisphere winter storm track modes. *Tellus*, **59A**, 599–617.
- Fyfe, J. C., 2003: Extratropical Southern Hemisphere cyclones: Harbingers of climate change? *J. Climate*, **16**, 2802–2805.
- , N. P. Gillett, and G. J. Marshall, 2012: Human influence on extratropical Southern Hemisphere summer precipitation. *Geophys. Res. Lett.*, **39**, L23711, doi:10.1029/2012GL054199.
- Garreaud, R. D., and J. M. Wallace, 1998: Summertime incursions of midlatitude air into subtropical and tropical South America. *Mon. Wea. Rev.*, **126**, 2713–2733.
- , and D. S. Battisti, 1999: Interannual (ENSO) and interdecadal (ENSO-like) variability in the Southern Hemisphere tropospheric circulation. *J. Climate*, **12**, 2113–2123.
- Gillett, N. P., J. C. Fyfe, and D. E. Parker, 2013: Attribution of observed sea level pressure trends to greenhouse gas, aerosol, and ozone changes. *Geophys. Res. Lett.*, **40**, 2302–2306, doi:10.1002/grl.50500.
- Hobbs, W. R., and M. N. Raphael, 2007: A representative time-series for the Southern Hemisphere zonal wave 1. *Geophys. Res. Lett.*, **34**, L05702, doi:10.1029/2006GL028740.
- Hoskins, B. J., and K. I. Hodges, 2005: A new perspective on Southern Hemisphere storm tracks. *J. Climate*, **18**, 4108–4129.
- Kang, S. M., L. M. Polvani, J. C. Fyfe, and M. Sigmon, 2011: Impact of polar ozone depletion on subtropical precipitation. *Science*, **332**, 951–954.
- Liebmann, B., and Coauthors, 2004: An observed trend in central South American precipitation. *J. Climate*, **17**, 4357–4367.
- Marshall, G. J., 2003: Trends in the southern annular mode from observations and reanalyses. *J. Climate*, **16**, 4134–4143.
- Mo, K. C., and J. N. Paegle, 2001: The Pacific–South American modes and their downstream effects. *Int. J. Climatol.*, **21**, 1211–1229, doi:10.1002/joc.685.
- Pezza, A., I. Simmonds, and J. A. Renwick, 2007: Southern Hemisphere cyclones and anticyclones: Recent trends and links with decadal variability in the Pacific Ocean. *Int. J. Climatol.*, **27**, 1403–1419.
- Purich, A., T. Cowan, S. Min, and W. Cai, 2013: Autumn precipitation trends over Southern Hemisphere midlatitudes as simulated by CMIP5 models. *J. Climate*, **26**, 8341–8356.
- Raphael, M., 2003: Recent, large-scale changes in the extratropical Southern Hemisphere atmospheric circulation. *J. Climate*, **16**, 2915–2924.
- Seneviratne, S. I., and Coauthors, 2012: Changes in climate extremes and their impacts on the natural physical environment. *Managing the Risks of Extreme Events and Disasters to Advance Climate Change Adaptation*, C. B. Field et al., Eds., Cambridge University Press, 109–230.
- Silvestri, G. E., and C. S. Vera, 2003: Antarctic Oscillation signal on precipitation anomalies over southeastern South America. *Geophys. Res. Lett.*, **30**, 2115, doi:10.1029/2003GL018277.
- Simmonds, I., and K. Keay, 2000: Variability of Southern Hemisphere extratropical cyclone behavior, 1958–97. *J. Climate*, **13**, 550–561.
- Solman, S., and I. Orlanski, 2010: Subpolar high anomaly preconditioning precipitation over South America. *J. Atmos. Sci.*, **67**, 1526–1542.
- Taschetto, A., and M. H. England, 2009: An analysis of late twentieth century trends in Australian rainfall. *Int. J. Climatol.*, **29**, 791–807, doi:10.1002/joc.1736.
- Thompson, D. W. J., and S. Solomon, 2002: Interpretation of recent Southern Hemisphere climate change. *Science*, **296**, 895–899, doi:10.1126/science.1069270.
- Uppala, S. M., and Coauthors, 2005: The ERA-40 Re-Analysis. *Quart. J. Roy. Meteor. Soc.*, **131**, 2961–3012.
- Vera, C., 2003: Interannual and interdecadal variability of atmospheric synoptic-scale activity in the Southern Hemisphere. *J. Geophys. Res.*, **108**, 8077, doi:10.1029/2000JC000406.
- , P. K. Vigiariolo, and E. H. Berbery, 2002: Cold season synoptic-scale waves over subtropical South America. *Mon. Wea. Rev.*, **130**, 684–699.
- Wang, X. L., V. R. Swail, and F. W. Zwiers, 2006: Climatology and changes of extratropical cyclone activity: Comparison of ERA-40 with NCEP–NCAR reanalysis for 1958–2001. *J. Climate*, **19**, 3145–3166.